JOURNAL OF THERMOPHYSICS AND HEAT TRANSFER
Vol. 7, No. 4, Oct.–Dec. 1993

Technical Notes

TECHNICAL NOTES are short manuscripts describing new developments or important results of a preliminary nature. These Notes cannot exceed 6 manuscript pages and 3 figures; a page of text may be substituted for a figure and vice versa. After informal review by the editors, they may be published within a few months of the date of receipt. Style requirements are the same as for regular contributions (see inside back cover).

Transient Free Convection Between Two Concentric Spheres Filled with a Porous Medium

I. Pop*
University of Cluj, Cluj CP 253, Romania
D. B. Ingham†
University of Leeds,
Leeds LS2 9JT, England, United Kingdom
and
P. Cheng‡
University of Hawaii at Manoa,
Honolulu, Hawaii 96822

Nomenclature

$C_1^{(i)}$, $C_1^{(0)}$ = constants, Eqs. (8)
f_0, f_1, f_2 = functions, Eqs. (8)
g = acceleration due to gravity
K = permeability
k = effective thermal conductivity
R = radii ratio, R_0/R_i
R_i = radius of the inner sphere
R_o = radius of the outer sphere
Ra = Rayleigh number, $\rho g\beta K\Delta TR_i/(\mu\alpha)$
r = radial coordinate, r'/R_i
r_c = radius of the circular streamline, Eq. (9)
r_v = radius of the circle for tangential velocity, Eq. (11)
T = dimensionless temperature, $(T' - T'_f)/\Delta T$
T_f = initial temperature
T_i = nondimensional temperature of the inner cylinder, $(T'_i - T'_f)/\Delta T$
T_o = nondimensional temperature of the outer cylinder, $(T'_o - T'_f)/\Delta T = T_i - 1$
t = time, $t'/(\sigma t_0)$
t^* = time, $\alpha t'/(\sigma R_i^2)$
t_0 = characteristic time
U = characteristic speed, $\rho g\beta K\Delta T/\mu$
α = effective thermal diffusively
α^* = parameter, $(\varepsilon Ra)^{-1}$
β = coefficient of thermal expansion
ΔT = temperature difference, $T'_i - T'_o$
ε = parameter, Ut_0/R_i
η = similarity variable, $(r - 1)/(2t^{*1/2})$
θ^* = angular coordinate
μ = fluid viscosity
ξ = similarity variable, $(R - r)/(2t^{*1/2})$
ρ = density
σ = ratio of heat capacity of the saturated porous medium to that of the fluid
ϕ = azimuthal coordinate
ψ = stream function, $\psi'/(\alpha Ra)$

Subscripts
c = composite
w = value at the wall

Superscripts
$'$ = dimensional variable
c = core region
i = inner boundary layer
0 = outer boundary layer
$-$ = average quantity

Received June 23, 1992; revision received Oct. 19, 1992; accepted for publication Oct. 22, 1992.

*Professor, Faculty of Mathematics.
†Professor, Department of Applied Mathematical Studies.
‡Professor, Department of Mechanical Engineering.

Introduction

OWING to its wide applications in geophysics and in various engineering devices, heat and fluid flow within fluid-saturated porous medium has been extensively studied over the years.[1,2] This includes the utilization of geothermal energy, the control of pollutant spread in groundwater, as well as the design of nuclear reactors, compact heat exchangers, solar power collectors, and high-performance insulation for buildings. Heat transfer by free convection between two cylinders (horizontal or vertical) and spheres filled with porous media is of fundamental importance in many of these applications. A review of the literature shows that cylindrical porous geometries have probably been studied more and are better understood.[3–9] In contrast, the spherical porous geometry[10] deserves further treatment and has not been examined as rigorously as cylindrical geometries. Furthermore, the governing equations are very complex in spherical coordinates.

Recently, Sano[11] considered the problem of transient-free convection between two horizonal concentric cylinders containing a Newtonian fluid. He was able to predict analytically the existence of three distinct regions in the initial flowfield, and four different patterns of motion may be distinguished, corresponding to four different types of thermal boundary conditions. This article has been recently extended to the case of a horizontal annulus filled with a porous medium by Pop et al.[12]

The aim of this Note is to describe the initial phase of transient-free convection between two concentric spheres filled with a porous medium. Short-time solutions to the momentum (Darcy) and energy equations are obtained analytically using the method of matched asymptotic expansion (see Pop et al.[12]).

Analysis

Consider the free convection between two convective spheres filled with a porous medium. It is assumed, that initially, the fluid between the spheres is at rest and has the uniform temperature T'_f, and that the transient flow is caused by step changes in the surface temperature of the inner and outer spheres from T'_f to T'_i and T'_o, respectively. In spherical coordinates, with the origin at the center of the spheres, the

equations governing the initial motion with the Darcy and Boussinesq approximations can be written in nondimensional form as

$$D^2\psi = -r\sin\theta^*\left(\frac{\partial T}{\partial r}\sin\theta^* + \frac{\partial T}{\partial\theta^*}\frac{\cos\theta^*}{r}\right) \quad (1)$$

$$\frac{\partial T}{\partial t} + \frac{\varepsilon}{r^2\sin\theta^*}\frac{\partial(T,\psi)}{\partial(r,\theta^*)} = \alpha^*\varepsilon^2\nabla^2 T \quad (2)$$

along with the initial and boundary conditions

$$t < 0: \quad \psi = T = 0 \quad (3a)$$

$$t \geq 0: \begin{cases} \psi = 0, \quad T = T_i \quad \text{at} \quad r = 1 & (3b) \\ \psi = 0, \quad T = T_o \quad \text{at} \quad r = R & (3c) \end{cases}$$

where

$$D^2 = \frac{\partial^2}{\partial r^2} - \frac{\cot\theta^*}{r^2}\frac{\partial}{\partial\theta^*} + \frac{1}{r^2}\frac{\partial^2}{\partial\theta^{*2}} \quad (4a)$$

$$\nabla^2 = \frac{\partial^2}{\partial r^2} + \frac{2}{r}\frac{\partial}{\partial r} + \frac{\cot\theta^*}{r^2}\frac{\partial}{\partial\theta^*} + \frac{1}{r^2}\frac{\partial^2}{\partial\theta^{*2}} \quad (4b)$$

Solutions to Eqs. (1–3) are sought as perturbation expansions in powers of the small parameter ε, but for α^* being 0(1). The flowfield between the spheres is divided into three regions: 1) an inner boundary-layer near the inner sphere; 2) an outer boundary-layer near the outer sphere; and 3) a core region between the two boundary layers. These inner, outer, and core flowfields are determined simultaneously. The inner and outer solutions, solved in the stretched coordinates, satisfy the boundary conditions on the spheres. They are then expressed in intermediate coordinates and matched. The procedure parallels those of previous studies by Sano[11] and Pop et al.[12] and will not be considered in detail here. Only the composite solution will be shown in the next section.

Results and Discussion

The composite solution is the inner solution plus the outer solution plus the core solution, minus the terms which are common to the three solutions. The solution valid for the whole field is then

$$\begin{aligned}
\psi_c = {} & 2t^{*1/2}T_i\left[-\eta\,\mathrm{erfc}(\eta) + \frac{1}{\sqrt{\pi}}e^{-\eta^2}\right]\sin^2\theta \\
& + 2t^{*1/2}RT_o\left[\xi\,\mathrm{erfc}(\xi) - \frac{1}{\sqrt{\pi}}e^{-\xi^2}\right]\sin^2\theta \\
& + \frac{2t^{*1/2}}{\sqrt{\pi}(R^3-1)}\left[(T_i + R^2T_o)r^2 - R^2(T_o + RT_i)r^{-1}\right] \\
& \times \sin^2\theta + t^*T_i\left[(1+2\eta^2)\mathrm{erfc}(\eta) - \frac{2}{\sqrt{\pi}}\eta e^{-\eta^2}\right]\sin^2\theta \\
& + t^*T_o\left[(1+2\xi^2)\mathrm{erfc}(\xi) - \frac{2}{\sqrt{\pi}}\xi e^{-\xi^2}\right]\sin^2\theta \\
& + \frac{t^*}{R^3-1}\left[(T_i - RT_o)r^2 + R(T_o - R^2T_i)r^{-1}\right]\sin^2\theta \\
& - 2t^{*3/2}T_i\left[(\eta+2\eta^3)\mathrm{erfc}(\eta) - \frac{2}{\sqrt{\pi}}\eta^2 e^{-\eta^2}\right]\sin^2\theta \\
& + 2t^{*3/2}R^{-1}T_o\left[(\xi+2\xi^3)\mathrm{erfc}(\xi) - \frac{2}{\sqrt{\pi}}\xi^2 e^{-\xi^2}\right]\sin^2\theta \\
& + 2|Ra|t^{*3/2}T_i^2\left[f_2(\eta) + \frac{2}{3\sqrt{\pi}}\left(\frac{4\sqrt{2}-9}{2} + \frac{8}{3\pi}\right)\right] \\
& \times \sin^2\theta\cos\theta - 2|Ra|t^{*3/2}T_0^2 \\
& \times \left[f_2(\xi) + \frac{2}{3\sqrt{\pi}}\left(\frac{4\sqrt{2}-9}{2} + \frac{8}{3\pi}\right)\right]\sin^2\theta\cos\theta \\
& + \frac{4|Ra|t^{*3/2}}{3\sqrt{\pi}(R^5-1)}\left(\frac{4\sqrt{2}-9}{2} + \frac{8}{3\pi}\right) \\
& \times \left[(T_i^2 + R^2T_o^2)r^3 - R^2(T_o^2 + R^3T_i^2)r^{-2}\right]\sin^2\theta\cos\theta \\
& + \text{h.o.t.} \qquad (5)
\end{aligned}$$

$$\begin{aligned}
V_c = {} & T_i\,\mathrm{erfc}(\eta)\sin\theta + T_o\,\mathrm{erfc}(\xi)\sin\theta \\
& - \frac{2t^{*1/2}}{\sqrt{\pi}(R^3-1)}\left[2(T_i + R^2T_o) + R^2(T_o + RT_i)r^{-3}\right] \\
& \times \sin\theta - 2t^{*1/2}T_i\left[2\eta\,\mathrm{erfc}(\eta) - \frac{1}{\sqrt{\pi}}e^{-\eta^2}\right]\sin\theta \\
& + 2t^{*1/2}R^{-1}T_o\left[2\xi\,\mathrm{erfc}(\xi) - \frac{1}{\sqrt{\pi}}e^{-\xi^2}\right]\sin\theta \\
& - \frac{t^*}{R^3-1}\left[2(T_i - RT_o) - R(T_o - R^2T_i)r^{-3}\right]\sin\theta \\
& + t^*T_i\left[(1+14\eta^2)\mathrm{erfc}(\eta) - \frac{10}{\sqrt{\pi}}\eta e^{-\eta^2}\right]\sin\theta \\
& + t^*R^{-2}T_o\left[(1+14\xi^2)\mathrm{erfc}(\xi) - \frac{10}{\sqrt{\pi}}\xi e^{-\xi^2}\right]\sin\theta \\
& - |Ra|t^*T_i^2 f_0(\eta)\sin\theta\cos\theta - |Ra|t^*R^{-1}T_o^2 f_0 \\
& \times (\xi)\sin\theta\cos\theta - \frac{4|\mathrm{Ra}|t^{*3/2}}{3\sqrt{\pi}(R^5-1)}\left(\frac{4\sqrt{2}-9}{2} + \frac{8}{3\pi}\right) \\
& \times \left[3(T_i^2 + R^2T_o^2)r + 2R^2(T_o^2 + R^3T_i^2)r^{-4}\right]\sin\theta\cos\theta \\
& + \text{h.o.t.} \qquad (6)
\end{aligned}$$

$$\begin{aligned}
T_c = {} & T_i\,\mathrm{erfc}(\eta) + T_o\,\mathrm{erfc}(\xi) - 2t^{*1/2}T_i\eta\,\mathrm{erfc}(\eta) \\
& + 2t^{*1/2}R^{-1}T_o\xi\,\mathrm{erfc}(\xi) + 4t^*T_i\eta^2\,\mathrm{erfc}(\eta) \\
& + 4t^*R^{-2}T_o\xi^2\,\mathrm{erfc}(\xi) - t^*|Ra|T_i^2 f_0(\eta)\cos\theta \\
& - t^*|Ra|R^{-1}T_o^2 f_0(\xi)\cos\theta + t^{*3/2}|Ra|T_i^2 \\
& \times \left[f_1(\eta) + \frac{48}{5\pi}C_1^{(i)}\eta e^{-\eta^2}\right]\cos\theta - t^{*3/2}|Ra|R^{-2}T_o^2 \\
& \times \left[f_1(\xi) - \frac{48}{5\pi}C_1^{(0)}\xi e^{-\xi^2}\right]\cos\theta + \text{h.o.t.} \qquad (7)
\end{aligned}$$

where ψ_c, V_c, and T_c are the composite stream function, tangential velocity, and temperature, respectively. In the above equations we have adopted the notation.

$$C_1^{(i)} = \frac{1 + R^2(T_o/T_i)}{R^3 - 1} \quad (8a)$$

$$C_1^{(0)} = \frac{R(R^2 + T_i/T_o)}{R^3 - 1} \quad (8b)$$

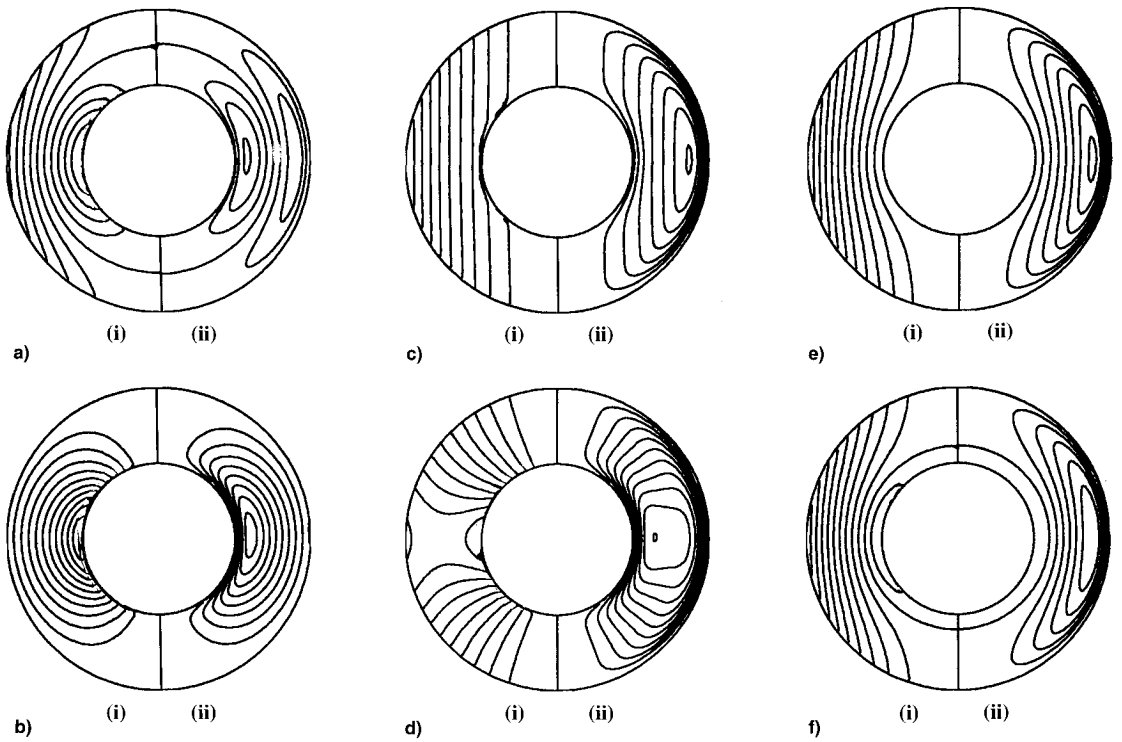

Fig. 1 Streamline patterns for a) $R = 2$, $|Ra| = 10$, $T_i = 2$ [(i) $t^* \to 0$, (ii) $t^* = 0.01$]; b) $R = 2$, $|Ra| = 10$, $T_i = 1$ [(i) $t^* \to 0$, (ii) $t^* = 0.01$]; c) $R = 2$, $|Ra| = 10$, $T_i = \frac{7}{22}$ [(i) $t^* \to 0$, (ii) $t^* = 0.01$]; d) $R = 2$, $|Ra| = 10$, $T_i = \frac{15}{22}$ [(i) $t^* \to 0$, (ii) $t^* = 0.01$]; e) $R = 2$, $|Ra| = 10$, $T_i = 0$ [(i) $t^* \to 0$, (ii) $t^* = 0.01$]; and f) $R = 2$, $|Ra| = 10$, $T_i = -1$ [(i) $t^* \to 0$, (ii) $t^* = 0.01$].

$$f_0(x) = (1 + 2x^2)\text{erfc}^2(x) - \frac{2}{\sqrt{\pi}} xe^{-x^2}\,\text{erfc}(x) + \frac{8}{3\pi} e^{-x^2} - \left(1 + \frac{8}{3\pi}\right)\left[(1 + 2x^2)\text{erfc}(x) - \frac{2}{\sqrt{\pi}} xe^{-x^2}\right] \tag{8c}$$

$$f_1(x) = 2\left(x + \frac{10}{3}x^3\right)\text{erfc}^2(x) - \frac{2}{3\sqrt{\pi}}\left[4 + (4x^2 - 5)e^{-x^2}\right]\text{erfc}(x) - \frac{4}{\pi} xe^{-2x^2} + \frac{224}{15\pi} xe^{-x^2} - \frac{1}{\sqrt{\pi}} e^{-x^2} - \frac{1}{6}\left[(3x + 2x^3)\text{erfc}(x) - \frac{2}{\sqrt{\pi}}(1 + x^2)e^{-x^2}\right] - 2\left(1 + \frac{8}{3\pi}\right)\left[(x + 2x^3)\text{erfc}(x) - \frac{1}{\sqrt{\pi}} x^2 e^{-x^2}\right] \tag{8d}$$

$$f_2(x) = \left(x + \frac{2}{3}x^3\right)\text{erfc}^2(x) - \frac{1}{3\sqrt{\pi}}[4 + (7 + 4x^2)e^{-x^2}] \times \text{erfc}(x) + \frac{2}{3\pi} xe^{-2x^2} + \frac{8}{3\sqrt{2\pi}}\text{erfc}(\sqrt{2}x) - \frac{2}{3\sqrt{\pi}}\left(\frac{4\sqrt{2} - 9}{2} + \frac{8}{3\pi}\right) - \left(1 + \frac{8}{3\pi}\right) \times \left[\left(x + \frac{2}{3}x^3\right)\text{erfc}(x) - \frac{2}{3\sqrt{\pi}}(1 + x^2)e^{-x^2}\right] \tag{8e}$$

As in the work by Pop et al.[12] on the transient-free convection between two horizontal concentric cylinders filled with a porous medium, the effect of the change in temperature is felt in the core flow after a time $0(t^{*1/2})$, whereas for the corresponding flow in a nonporous media, it takes $0(t^{*3/2})$. This faster transmission of information is a fact of porous medium, and therefore, the results are as expected.

In the limit as $t^* \to 0$, all the results become independent of the Rayleigh number and there exists a circular streamline of radius

$$r_c = \sqrt[3]{R^2\{[(1 + R)T_i - 1]/[(1 + R^2)T_i - R^2]\}} \tag{9}$$

for $T_i > 1$ and $T_i < 0$. This result is again what we would have physically expected. Since if $T_i > 1$ (<0), both the spheres are impulsively heated (cooled) to a constant temperature in excess (below) of that of the surrounding fluid, and hence, the fluid flow rises (falls) near the surfaces of the spheres and from continuity fluid flow must fall (rise) in the core of the flow, i.e., near $r = r_c$. In order to illustrate these types of flows, Fig. 1 shows the streamlines as $t^* \to 0$ and $t^* = 0.01$ for $R = 2$, $Ra = 10$, and $T_i = 2$, 1, $\frac{7}{22}$, $\frac{15}{22}$, 0, and -1. When $0 < T_i < 1$, i.e., $-1 < T_o < 0$, then the inner sphere is heated and the outer sphere cooled. Therefore, the flow will rise near the outer sphere and only a single recirculatory flow will be produced, see part(i) in Figs. 1c and 1d.

It is interesting to note that in Figs. 1b–e, only one recirculating flow has been generated since $0 < T_i < 1$, but the nature of the flow is quite distinct for $T_i = \frac{15}{22}$. The reason for this may be found from examining the leading-order core velocity, i.e.

$$V_c = -[2t^{*1/2}/(R^3 - 1)\sqrt{\pi}][2(T_i + R^2T_o) + R^2(T_o + RT_i)r^{-3}]\sin\theta \tag{10}$$

which shows that there is a circle of radius

$$r_v = \sqrt[3]{(R^2/2)\{[(1 + R)T_i - 1]/[(1 + R^2)T_i - R^2]\}} \tag{11}$$

on which this core velocity is zero, provided that $1 \leq r_v \leq R$. On manipulation of these inequalities we find that the zero-order core velocity is zero when

$$\frac{3R^2}{2 + 3R^2 + R^3} \leq T_i \leq \frac{1 + 2R^3}{1 + 3R + 2R^3} \tag{12}$$

which, for example, reduces to

$$\begin{aligned} R &\to \infty \quad & 0 &\leq T_i \leq 1 \\ R &= 4 \quad & \tfrac{12}{57} &\leq T_i \leq \tfrac{66}{77} \\ R &= 2 \quad & \tfrac{6}{11} &\leq T_i \leq \tfrac{17}{23} \\ R &= \tfrac{3}{2} \quad & \tfrac{54}{97} &\leq T_i \leq \tfrac{31}{49} \\ R &\to 1 \quad & T_i &= \tfrac{1}{2} \end{aligned} \tag{13}$$

Therefore, there is a finite range of values of T_i for which the zero-order core velocity is zero for all values of R, but as $R \to 1$, $T_i \to \frac{1}{2}$.

It is observed from all (i) in Fig. 1, that as $t^* \to 0$, the boundary layers on $r = 1$ and $r = R$ are of zero thickness, and then as t^* increases, these boundary layers increase in thickness and diffuse into the core flow. Furthermore, it is seen that when $T_i = 1$ ($T_i = 0$), i.e., $T_o = 0$ ($T_i = -1$), then the boundary layer on the outer (inner) sphere has not been changed from that of the original core temperature.

References

[1]Cheng, P., "Geothermal Heat Transfer," *Handbook of Heat Transfer Applications*, edited by W. M. Rohsenow, J. P. Hartnett, and E. N. Ganic, 2nd ed., McGraw-Hill, New York, 1985, Chap. 11.

[2]Bejan, A., "Convective Heat Transfer in Porous Media," *Handbook of Single-Phase Convective Heat Transfer*, edited by S. Kakac, R. K. Shah, and W. Aung, Wiley, New York, 1987, Chap. 16.

[3]Caltagirone, J. P., "Thermoconvective Instabilities in a Porous Medium Bounded by Two Concentric Horizontal Cylinders," *Journal of Fluid Mechanics*, Vol. 76, Pt. 2, 1976, pp. 337–362.

[4]Bejan, A., and Tien, C. L., "Natural Convection in Horizontal Cylinders with Different End Temperatures," *International Journal of Heat and Mass Transfer*, Vol. 22, No. 6, 1979, pp. 919–927.

[5]Havstad, M. A., and Burns, P. J., "Convective Heat Transfer in Vertical Cylindrical Annuli Filled with a Porous Medium," *International Journal of Heat and Mass Transfer*, Vol. 25, No. 11, 1982, pp. 1755–1765.

[6]Vasseur, P., Nguyen, T. H., Robilard, L., and Thi, V. K. T., "Natural Convection Between Horizontal Concentric Cylinders Filled with a Porous Layer with Internal Heat Generation," *International Journal of Heat and Mass Transfer*, Vol. 27, No. 3, 1984, pp. 337–349.

[7]Bau, H. H., "Low Rayleigh Number Thermal Convection in a Saturated Porous Medium Bounded by Two Horizontal, Eccentric Cylinders," *Journal of Heat Transfer*, Vol. 106, No. 1, 1984, pp. 166–175.

[8]Himasekhar, K., and Bau, H. H., "Two Dimensional Bifurcation Phenomena in Thermal Convection in Horizontal, Concentric Annuli Containing Saturated Porous Media," *Journal of Fluid Mechanics*, Vol. 187, Pt. 2, 1988, pp. 267–300.

[9]Kimura, S., and Pop, I., "Conjugate Natural Convection Between Horizontal Concentric Cylinders Filled with a Porous Medium," *Wärme- und Stoffübertragung*, Vol. 27, No. 1, 1992, pp. 85–91.

[10]Burns, J. P., and Tien, C. L., "Natural Convection in Porous Media Bounded by Concentric Spheres and Horizontal Cylinders," *International Journal of Heat and Mass Transfer*, Vol. 22, No. 6, 1979, pp. 929–939.

[11]Sano, T., "Transient Natural Convection Between Horizontal Concentric Cylinders," *Fluid Dynamics Research*, Vol. 1, No. 1, 1986, pp. 33–47.

[12]Pop, I., Ingham, D. B., and Cheng, P., "Transient Natural Convection in a Horizontal Concentric Annulus Filled with a Porous Medium," *Journal of Heat Transfer*, Vol. 114, No. 4, 1992, pp. 990–997.

Calculation of Real-Gas Effects on Airfoil Aerodynamic Characteristics

Chul Park*
NASA Ames Research Center, Moffett Field, California 94035
and
Seokkwan Yoon†
MCAT Institute, Moffett Field, California 94035

Nomenclature

a/a = angle of attack, deg
C_D = drag coefficient
C_L = lift coefficient
CP = center of pressure
V = flight velocity, km/s
γ = specific heat ratio

Introduction

ELLIPSES of thickness ratio varying from 5 to 15% and the airfoil for the wings of the Space Shuttle Orbiter are considered for this study. Their exact geometries are given in Ref. 1. Chord lengths for these geometries are varied between 2–50 m. Two-dimensional, chemically reacting flowfields around these geometries are calculated in the present work using the computer codes CENS2H and CENS2D described in Refs. 2 and 3. The CENS2H code assumes air to consist of five neutral species N, O, NO, N_2, and O_2, and accounts for thermal and chemical nonequilibria in the shock layer, i.e., it uses a two-temperature reaction model. The CENS2D code is for an ideal gas of fixed γ ($= C_p/C_v$). Freestream velocity is varied between 3–7 km/s for the present calculation. The freestream density is varied as 8×10^{-6}, 4×10^{-5}, 2×10^{-4}, and 10^{-3} kg/m^3, corresponding approximately to the flight altitudes of 85, 74, 63, and 50 km, respectively. Angle of attack is varied as 20, 30, and 40 deg. The rate parameters given in Refs. 2 and 3, which are to be referred to as the standard rates, are used in most of the present calculations.

Convergence performance of these codes has been examined in Refs. 2 and 3 for an Apollo-shaped blunt body and a slender ellipse, respectively. One-temperature solutions can be obtained using CENS2H by setting the vibrational relaxation times to be very short.[2,3] Near equilibrium solutions can be obtained also using CENS2H by setting reaction rates to be very large.[2,3] It was shown in Ref. 2 that the aerodynamic characteristics of near-equilibrium flows can be represented approximately by those of ideal-gas flows of fixed γ less than 1.4.

Algebraically-generated grids of $110 \times 80 = 8800$ node points are used for the present calculations. Lift, drag, and moments are calculated accounting only for pressure, neglecting skin friction. The shift in the CP location is determined as the difference between the location of the CP for the reacting flow and that of the perfect-gas ($\gamma = 1.4$) flow. CP shift is represented as a percentage of the chord length.

Presented as Paper 90-1712 at the AIAA/ASME 5th Joint Thermophysics and Heat Transfer Conference, Seattle, WA, June 18–20, 1990; received Feb. 7, 1991; revision received Oct. 16, 1992; accepted for publication Nov. 18, 1992.

*Chief, Experimental Aerothermodynamics Section. Associate Fellow AIAA.

†Senior Scientist. Senior Member AIAA.